A SIMULATION OF DUCTILE FRACTURE IN A THREE-POINT BEND SPECIMEN USING A SOFTENING MATERIAL RESPONSE

Guo Chen Li* and I. C. Howard**

**Institute of Mechanics, Academia Sinica, Beijing, China*
***Department of Mechanical Engineering, University of Sheffield, England*

ABSTRACT

Previous work on the role of softening in the plastic response of ductile metals at large strains has been extended to include the effects of plastic dilatation. The influence of softening, both deviatoric and volumetric, on the crack tip field and on the initial stages of stable crack growth in a three-point bend specimen of A533B nuclear pressure vessel steel has been examined.

KEYWORDS

Plastic dilatation; constitutive equations for dilatant plastic flow; void growth; softening; crack growth.

INTRODUCTION

The importance of triaxial stress and its potential for producing plastic dilatation in ductile metals has attracted increasing interest. Experimental observation of the effect of hydrostatic stress on yielding (Spitzig and colleagues, 1976) and of the development of damage and voiding with strain (Iricibar and colleagues, 1980) have been complemented by theories of void growth (Rice and Tracey, 1969) and of the continuum effects of void growth on the yield function (Gurson, 1977). Many attempts have been made to include these effects into studies of the behaviour of material subjected to high triaxiality, and some of the different treatments that have been used include the work of Brown and colleagues (1980) who used Gurson's model to simulate the behaviour of notched tensile specimens and the work of Rousselier (1981) who included ductile fracture damage in his constitutive equations.

We propose an alternative to these approaches which appears to have certain attractive advantages. The constitutive equations are relatively simple, and contain moduli and material parameters whose values are ascertainable by comparing the results of model studies with experimental tests on plain and notched bars. Softening is an essential component of these equations and it has the advantage of allowing crack growth in a simple, natural way. This and other features of this approach to ductile deformation and fracture, are illustrated by an analysis of a three-point bend specimen.

CONSTITUTIVE EQUATIONS

The generalization of the classical Prandtl-Reuss equations to finite strain used in our previous studies (Li and Howard, 1983a, 1983b) of ductile fracture has been extended to include the effects of plastic dilatation by the addition of a term that accounts for the development of a volumetric plastic strain rate. The mixed tensorial form of the constitutive equations for the strain rate is

$$D^i_j = \frac{1}{E}\left[(1+\nu)\frac{\mathcal{D}\tau^i_j}{\mathcal{D}t} - \nu\delta^i_j\frac{\mathcal{D}\tau^k_k}{\mathcal{D}t}\right] + \alpha\frac{9}{4E^{(p)}_{te}}\frac{s^i_j s^k_\ell}{\sigma_e^2}\frac{\mathcal{D}\tau^\ell_k}{\mathcal{D}t} + \frac{\alpha}{3E^{(p)}_{tm}}\delta^i_j\frac{\mathcal{D}\tau^k_k}{\mathcal{D}t} \tag{1}$$

in which $\mathcal{D}\tau^i_j/\mathcal{D}t$ is the Jaumann rate of Kirchhoff stress, s^i_j and σ_e are the deviatoric Cauchy stress and its equivalent stress and $E^{(p)}_{te}$ is the usual (deviatoric) plastic tangent modulus. The parameter α is zero if the material is elastic and unity if it is plastic. The first three terms in (1) are a natural extension of Prandtl-Reuss theory. In the fourth, which represents the effect of plastic dilatation, we define the volumetric tangent modulus as

$$E^{(p)}_{tm} = \frac{\mathcal{D}\tau^k_k}{\mathcal{D}t}\bigg/ D^k_k \tag{2}$$

where D^k_k is three times the mean strain rate. The inverse of equation (1) is

$$\frac{\mathcal{D}\tau^i_j}{\mathcal{D}t} = \frac{E}{(1+\nu)}\left[D^i_j + \frac{\nu\delta^i_j D^k_k}{(1-2\nu) + \alpha E/E^{(p)}_{tm}} - \alpha\frac{E}{3E^{(p)}_{tm}}\frac{\delta^i_j D^k_k}{(1-2\nu + \alpha E/E^{(p)}_{tm})} - \alpha\frac{9E}{4E^{(p)}_{te}}\frac{s^i_j}{\sigma_e^2}\frac{s^k_\ell s^\ell_k}{(1+\nu + \alpha 3E/2E^{(p)}_{te})}\right] \tag{3}$$

Both the plastic moduli $E^{(p)}_{te}$ and $E^{(p)}_{tm}$ are positive whilst the material hardens and we also allow the possibility of negative values corresponding to material softening if certain conditions are met. Our previous work suggests that the inception of softening in A533B steel is controlled by stress. Accordingly, the equivalent stress σ_e - strain ε_e curve softens when the condition

$$\sigma_m + \lambda_e\sigma_e = \sigma_{ce} \tag{4}$$

is reached. Softening of the mean stress σ_m - strain ε_m curve occurs when

$$\sigma_m + \lambda_m\sigma_e = \sigma_{cm} \tag{5}$$

The determination of the four material constants λ_e, λ_m, σ_{ce} and σ_{cm} and the two plastic tangent moduli was accomplished with the aid of simulation studies. The details of this will be reported elsewhere but, briefly, the deviatoric tangent modulus $E^{(p)}_{te}$ was obtained by simulating a standard tensile test (Li, 1983), the values

$$\lambda_e = 1.40\ ,\quad \lambda_m = 3.46\ ,\quad \frac{\sigma_{ce}}{\sigma_Y} = 3.4\ ,\quad \frac{\sigma_{cm}}{\sigma_Y} = 6.5$$

for the four material constants and the volumetric tangent modulus $E^{(p)}_{tm}$ were obtained from the results (Li and Howard, 1983a) of a cell model of void growth in A533B steel. The effects of differing amounts of softening and plasticity were investigated by changing the variables as in Table 1 to give five different material responses. For purposes of comparison, the material of case 4 corresponds most closely to the behaviour of A533B nuclear pressure vessel steel.

TABLE 1 Material Hardening and Softening Characteristics

Case	Softening $\frac{E}{E^{(p)}_{te}}$	Hardening $\frac{E}{E^{(p)}_{tm}}$	Softening $\frac{E}{E^{(p)}_{tm}}$
1	No	No	No
2	-400	No	No
3	-100	No	No
4	-100	0.2	-10
5	-100	0.5	-10

A DUCTILE FRACTURE ANALYSIS OF A THREE-POINT BEND SPECIMEN

A finite element analysis of the specimen was accomplished using constant plane-strain triangular elements with two meshes, A (268 nodes, 480 elements) and A′ (218 nodes, 380 elements); Fig. 1. The particular geometry investigated had L/W = 2 and a/W = 0.5. The computational method employed was an adaptation of that used previously (Li and Howard, 1983a, 1983b) in studies of ductile behaviour with the finite deformation being followed through the use of an up-dated Lagrangian formulation.

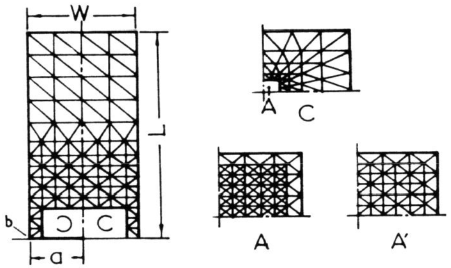

Fig. 1. The finite element meshes used in the calculations. Mesh A gives better refinement near the crack tip.

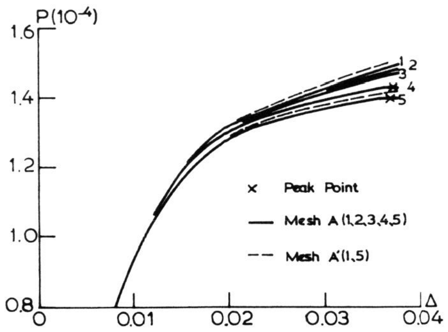

Fig. 2. Load deflection curves. P is the actual load normalized by EL and Δ is the actual deflection at point b of Fig. 1 normalized by W.

Fig. 2 shows how the differing softening responses affect the overall load-deflected records. The major qualitative difference in the curves is the appearance of a maximum in the load-deflection record in cases 4 and 5. Not only does softening reduce the load at which this occurs, it also reduces the deflection. A change of mesh does not significantly change the general trend of the curves but it does affect the point of occurrence of the maximum. The relationship between crack mouth opening and load point displacement is virtually unaffected by degree of softening or change of mesh.

As might have been expected, the local crack tip field depends strongly on the degree of softening, and this is borne out by the crack shapes shown in Fig. 3. Both softening and mesh refinement increase the CTOD. The stresses ahead of the crack tip are shown in Fig. 4, and it can be seen that softening reduces them to very small values over some distance (which depends on the degree of softening) ahead of the crack tip. Furthermore,

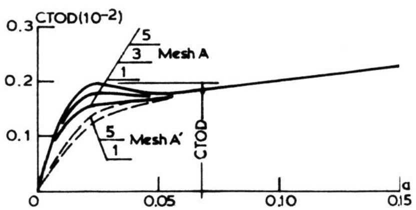

Fig. 3. Crack tip shapes at Δ = 0.0369. CTOD is the actual value normalized by L.

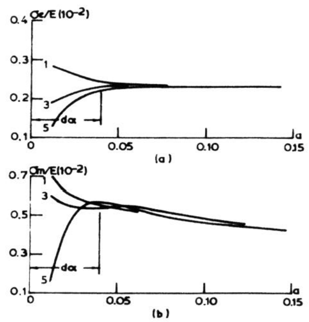

Fig. 4. Distribution of stress ahead of the crack tip at Δ = 0.0369

as is illustrated in Fig. 5 for the material of case 4, the softening is spread all around the crack tip, this being a continuum representation of the diffuse pattern of voiding that is often observed in micrographs of the material near the crack tip in ductile metals (for example, Shih and colleagues, 1979).

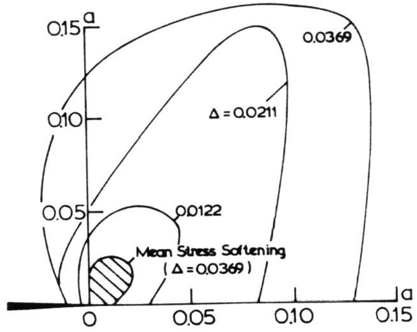

Fig. 5. The spread of softening around the crack tip for three positions of equivalent stress softening and one of mean stress.

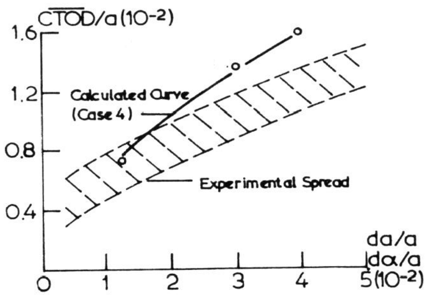

Fig. 6. Calculated resistance curve in comparison with experimental data.

As the specimen is deformed the region of softening at the crack tip grows and it is possible to identify a growth parameter dα, the extent of seriously softened material ahead of the tip. (The definition of dα is exemplified in Fig. 4). The results for case 4 material (which corresponds most closely to our previous simulations of the behaviour of A533B steel) are plotted in Fig. 6 as a resistance curve of CTOD as a function of dα and compared with the spread of measured resistance curves on compact tension specimens reported by Shih et al. (1979). Due to the uncertainty in the connection between our dα and the measured crack growth da and the approximation in specifying the matrix softening parameters of the void model on which the present work is based, the agreement is encouraging, at the very least.

CONCLUSIONS

This preliminary study has shown that it is possible to model the complex softening characteristics of real steels by relatively simple constitutive assumptions which are a logical extension of classical plasticity. In the present work the calibration of the constitutive equations was actually based on the analysis of a void model and the results of tests on plain and notched bars as given, for example, by Mackenzie, Hancock and Brown (1977) for different steels to the one studied here. Furthermore, the application of these constitutive equations to a simulation of deformation and growth at a crack tip in ductile material demonstrates the potential superiority of material softening as a modelling technique in comparison with node relaxation or tip shifting methods. In these, the material off the line of the crack retains the full stiffness of the hardening continuum in contradiction to the observations of voiding to the sides as well as ahead of a crack tip in ductile metals.

The attempt at predicting a crack growth resistance curve was done in terms of a parameter dα, the extent of serious material softening. The main reason for this choice instead of da, the region over which the material has effectively no stiffness, was that mesh A, the most refined mesh that could be easily analysed on the computers available to us, was not sufficiently refined. This meant that it was not possible to model accurately the large strain gradients that exist over microstructurally significant distances. These large strains were, in our computations, spread over large distances with the result that local crack tip softening was under-estimated. Our use of $d\alpha$ is an attempt to use an averaged softening response to compensate for the lack of precise detail in the present computations. Work towards a suitable mesh refinement that will allow reasonable modelling of the crack tip detail is under way.

REFERENCES

Brown, D. K., Hancock, J. W., Thomson, R. and Parks, D. M. (1980). Second Int. Conf. Numerical Methods in Fracture Mechanics, Swansea, U.K., (ed. D. R. J. Owen and A. R. Luxmoore), 309-325.

Gurson, A. L. (1977). *J. Eng. Mat. Technol.*, 99, 2-15.

Iricibar, R., le Roy, G. and Embury, J. D. (1980). *Metal Sci.*, 14, 337-343.

Li, G. C. (1983). *Int. J. Mech. Sci.*, 25, 47-57.

Li, G. C. and Howard, I. C. (1983a). *J. Mech. Phys. Solids*, 31, 85-102.

Li, G. C. and Howard, I. C. (1983b). In Int. Symposium on Fracture Mechanics, Beijing, China.

Mackenzie, A. C., Hancock, J. W. and Brown, D. K. (1977). *Engng. Fracture Mech.*, 9, 167-188.

Rice, J. R. and Tracey, D. M. (1969). *J. Mech. Phys. Solids*, 17, 201.

Rousselier, G. (1981). *Advances in Fracture Research*, ICF5, Cannes, France, (ed. D. Francois), 803-808.

Shih, C. F., de Lorenzi, H. G. and Andrews, W. R. (1979). *Elastic-Plastic Fracture*, ASTM STP 668 (ed. J. D. Landes, J. A. Begley and G. A. Clarke), 65-120.

Spitzig, W. A., Sober, R. J. and Richmond, O. (1976). *Met. Trans.*, 7A, 1703-1710.